

Platonic Entanglement

José I. Latorre^{1,2,3} and Germán Sierra⁴

¹ Quantum Research Centre, Technology Innovation Institute, Abu Dhabi, UAE.

² Center for Quantum Technologies, National University of Singapore, Singapore.

³ Qilimanjaro Quantum Tech, Barcelona, Spain

⁴ Instituto de Física Teórica UAM-CSIC, Universidad Autónoma de Madrid, Cantoblanco, Madrid, Spain.

(Dated: July 12, 2021)

We present a construction of highly entangled states defined on the topology of a platonic solid using tensor networks based on ancillary Absolute Maximally Entangled (AME) states. We illustrate the idea using the example of a quantum state based on AME(5,2) over a dodecahedron. We analyze the entropy of such states on many different partitions, and observe that they come on integer numbers and are almost maximal. We also observe that all platonic solids accept the construction of AME states based on Reed-Solomon codes since their number of facets, vertices and edges are always a prime number plus one.

ENTANGLEMENT AND TENSOR NETWORKS

The way multipartite entanglement is distributed over a quantum system is key to understand its emerging properties and, also, to devise good classical approximation strategies. A successful technology to achieve this dual goal is to represent quantum states as Tensor Networks (TN) [1, 2]. Indeed, TN provide one of the most powerful methods to represent classically a quantum state as a contraction of a series of tensors that take indices in an ancillary space.

It can be argued that TN attempt to describe a quantum state on a basis, different from the computational one, that rightly fits the entanglement properties of the system. Therefore, the technology of TN can be considered as a bona fide method to exploit the actual Kolmogorov complexity of a quantum state. They provide a most economical and adaptive description of quantum correlations.

Symmetries play a relevant role when choosing the appropriate TN to describe a quantum state. Most of condensed matter systems are defined on regular lattices, favoring the use of variants of TN such as Matrix Product States (MPS), or Projected Entangled Pair States (PEPS). At criticality, scale invariance is better captured by Multiscale Entanglement Renormalization Ansatz (MERA). In general, TN should adapt to the geometry dictated by the Hamiltonian of the system to implement the area law of the entanglement entropy. Although there are exceptions to this rule such as the rainbow state [3, 4].

It is perfectly correct to try TN which are not based on entangling only pairs of ancillary degrees of freedom. For instance, it may be advantageous to use TN based on three-body entangled units to describe triangular lattices. It can be argued that standard pair-wise entangling units, as in MPS and PEPs, will describe any entangling structure given a sufficient large ancillary dimension. This is indeed true, though such an approach may

not be the most efficient one. Some efforts have been devoted to analyze the properties of TN based on GHZ and W states to analyze frustrated systems [5]. Multipartite ancillary states have also been used to represent solutions to 3SAT problems [6].

A more sophisticated use of TN has been explored in the context of holography. There, TN based on Absolute Maximally Entangled (AME) [7]-[11] states are used to understand the emergence of space time and its holography properties [19–23].

Here, we consider the playful idea of building quantum states as the result of using AME states on topologies dictated by platonic solids. It is not obvious how such states can be built and, if so, how entanglement will be globally distributed. We shall find that large entanglement gets distributed if TN based on AMEs are used.

Let us also mention that the idea to choose the directions of quantum measurements according to the vertices of Platonic solids has been pursued in Ref [24]. Other works where Platonic solids have appeared in the context of Quantum Information can be found in references [25]-[29].

ABSOLUTE MAXIMALLY ENTANGLED STATES

Absolute Maximally Entangled [7]-[11] states, also called Perfect states [20], are defined as those multipartite quantum states whose reduced density matrices for any bi-partition are proportional to the identity. To be precise, given a state of n qudits, $|\psi\rangle \in \mathcal{H} = (\mathbb{C}^d)^{\otimes n}$, this state will be an AME state if all its reduced density matrices to a part A of m degrees of freedom, such that $\mathcal{A} \otimes \bar{\mathcal{A}} = \mathcal{H}$, carries a von Neumann entropy $S_{\mathcal{A}} = -\text{tr}(\rho_{\mathcal{A}} \log_2 \rho_{\mathcal{A}})$ given by

$$S_{\mathcal{A}} = m \log_2 d. \quad (1)$$

Qubits on vertices of a dodecahedron

To illustrate the construction of a platonic state, we consider the explicit example of a quantum state defined on the 20 vertices of a dodecahedron (see Fig. 1). The way to construct this state consists on producing a tensor network similar in spirit to the well-known PEPs, but using 5-qubit maximally entangled states instead of the usual maximally entangled pairs. The intuition behind this construction is that the AME(5,2) state may be able to distribute entanglement in a very efficient manner.

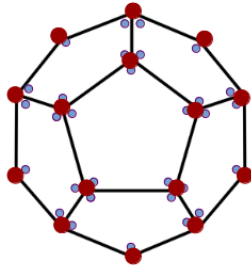


FIG. 1: A quantum state is defined on the vertices of a dodecahedron using an underlying tensor network. Each qubit is colored in red, whereas the ancillary degrees of freedom associated to 5-qubit maximally entangled states live on the pentagon faces and are represented in violet.

To be precise, the construction starts by filling the 12 pentagons of the dodecahedron with AME(5,2). Then, we define physical indices in each vertex using an agreement clause (see Fig. 2)

$$A_{\alpha\beta\gamma}^a = \delta_{\alpha}^a \delta_{\beta}^a \delta_{\gamma}^a. \quad (8)$$

That is, physical indices are made to coincide with the ancillary ones when all of them agree.

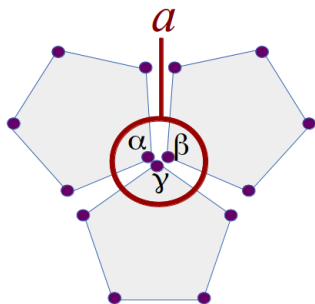


FIG. 2: Basic tensor assignment. Three pentagons meet at a vertex, each carrying ancillary indices α , β and γ , respectively. The tensor gets defined as $A_{\alpha\beta\gamma}^a = \delta_{\alpha}^a \delta_{\beta}^a \delta_{\gamma}^a$. Thus, the physical index a takes the value of the ancillae when they coincide, otherwise it is set to 0.

Since the basic tensor defining AME(5,2) in Eq. (4) is made of ± 1 , the global state we are defining on a dodeca-

hedron will carry all possible superpositions weighted with a plus or minus sign

$$|D_1\rangle = \frac{1}{\sqrt{2^{20}}} \sum_{i=0}^{2^{20}-1} c_i^D |i\rangle, \quad (9)$$

that is, all $c_i^D = 1$ or -1 .

The entanglement properties of the emerging state on a dodecahedron are non-trivial. The von Neumann entropy $S_A(D_1)$ for the state (4) and several block sizes $|A|$ are collected in Table II. We first observe that all bi-partitions, local or non-local, that involve 6 qubits or less carry maximal entanglement. For the bi-partitions of 10 vs 10 spins, the result for the entropy turns out to be always an integer number, and its maximal value of 10 is attainable.

$ A $	10	9	8	7	6	5	4	3	2	1
$S_A(D_1)$	7,8,9,10	7,8,9	7,8	6,7	6	5	4	3	2	1
$S_A(D_2)$	7,8	7,8	6,7,8	6,7	5,6	4,5	3,4	3	2	1

TABLE II: Entanglement entropies of AME(5,2) states (9) for various blocks of sizes $|A|$. $S(D_1)$ are for the state based on (4) and $S(D_2)$ are for the state using (10).

A rotational invariant AME(5,2) state

We observed above that the state (4) is not invariant under rotations of the qubits around the vertices of the pentagon. This implies that the resulting state over the dodecahedron depends on the specific choice of the AME(5,2) state for every pentagon. The analogy is that of a dodecahedron made of pentagons with different colors. The counting number of emerging states is an interesting but difficult problem that we shall not deal with here. Let us consider a rotational invariant AME(5,2) state given by [7]-[10]

$$\begin{aligned} |\text{AME}(5,2)\rangle = & \frac{1}{4} [|00000\rangle + |10010\rangle + |01001\rangle \\ & + |10100\rangle + |01010\rangle + |00101\rangle - |01111\rangle - |10111\rangle \\ & - |11011\rangle - |11101\rangle - |11110\rangle - |11000\rangle - |01100\rangle \\ & - |00110\rangle - |00011\rangle - |10001\rangle]. \end{aligned} \quad (10)$$

This state can be written as

$$\begin{aligned} |\text{AME}(5,2)\rangle = & \frac{1}{4} \sum_{\sum_j s_j \equiv 0 \pmod{2}} (-1)^{\sum_j s_j s_{j+1}} \\ & \times |s_1, \dots, s_5\rangle, \end{aligned} \quad (11)$$

where the sum runs over the spin configurations whose addition vanishes mod 2 (we take $s_6 = s_1$). Let us write

(11) as

$$|P\rangle = \frac{1}{4} \sum_{s_j, j \in P} (-1)^{\eta_P} |s_1, \dots, s_5\rangle, \quad \eta_P = \sum_{j \in P} s_j s_{j+1}, \quad (12)$$

where P denotes the pentagon whose vertices are occupied by the spins s_1, \dots, s_5 . The state over the dodecahedron constructed using (8) and (12), reads

$$|D_2\rangle = a_D \sum_{s_1, \dots, s_{20}} (-1)^{\eta_{P_1} + \dots + \eta_{P_{12}}} |s_1, \dots, s_{20}\rangle, \quad (13)$$

where the spins on each pentagon satisfy the neutrality condition

$$\sum_{i \in P_a} s_i = 0 \pmod{2}, \quad a = 1, \dots, 12. \quad (14)$$

a_D is the normalization constant of the state that is derived below. The assignment of vertices $i = 1, \dots, 20$, to pentagons P_a ($a = 1, \dots, 12$) is given in Fig. 3, that yields the neutrality conditions: $0 = s_1 + s_2 + s_3 + s_4 + s_5 = s_6 + s_7 + s_{15} + s_{16} + s_{20} = \dots$ where the equalities are defined mod 2. This is a set of 12 linearly independent

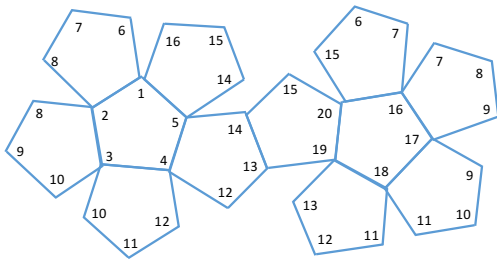


FIG. 3: Labels of the vertices of the dodecahedron.

equations for 20 variables that leaves 8 undetermined spins. Hence the state (13) is the linear superposition of 2^8 states out of the 2^{20} states of the computational basis that is normalized with $a_D = 1/\sqrt{2^8}$. Another feature of (13) is that the sign factor $(-1)^{\sum_a \eta_{P_a}}$ is equal to 1 for the 2^8 spin configurations that satisfy the neutrality conditions (14). Indeed, let's take a pair of spins, say s_i and s_j , on a link $\langle i, j \rangle$ on the dodecahedron. They give a factor $(-1)^{s_i s_j}$, associated to the pentagons sharing the link $\langle i, j \rangle$, and so the total contribution is 1. Hence the state (13) takes finally the form

$$|D_2\rangle = \frac{1}{\sqrt{2^8}} \sum'_{s_1, \dots, s_{20}} |s_1, \dots, s_{20}\rangle, \quad (15)$$

where \sum' denotes the sum over the spin configurations that satisfy (14).

The entanglement entropies $S_A(D_2)$ of (15) are collected in Table II for several blocks. Their maximal values are always lower than those of the state (9). An heuristic explanation is that (15) contains half of the states of (9) of the computational basis.

The entanglement entropies of (15) can be easily computed. Let A be a subset of $V_A \leq 10$ vertices. In general, not all the corresponding spins will be independent variables. For example, if A contains the sites $i = 1, 2, 3, 4, 5$ forming a pentagon, their spins must satisfy that $\sum_{i=1}^5 s_i = 0 \pmod{2}$, hence only 4 spins are independent. In this case the state (15) reads

$$|D\rangle = \frac{1}{\sqrt{2^4}} \sum'_{s_1, \dots, s_5} |s_1, \dots, s_5\rangle \otimes \frac{1}{\sqrt{2^4}} \sum'_{s_6, \dots, s_{20}} |s_6, \dots, s_{20}\rangle, \quad (16)$$

yielding an entropy $S_A = 4$. If the subset A contains n_A independent spin variables then (15) is decomposable as

$$|D\rangle = \frac{1}{\sqrt{2^{n_A}}} \sum'_{s_A} |s_A\rangle \otimes \frac{1}{\sqrt{2^{8-n_A}}} \sum'_{s_B} |s_B\rangle, \quad (17)$$

that gives an entropy $S_A = n_A$. Obviously, $n_A \leq 8$, which is the maximal attainable entropy. This can be achieved for $A = \{1, 2, 3, 4, 5, 16, 17, 18, 19, 20\}$ that contains two pentagons on opposite sides of the dodecahedron (see Fig.3).

Hovering qubits

A different arrangement of qubits based on AME networks can be obtained as follows. Every one of the 12 pentagons in the dodecahedron will carry an associated extra "hovering" qubit. We may think of it as placed in the center of the pentagon. This defines a unit cell made out of 6 qubits, five of them in the pentagon plus the hovering one. On each of these cells we introduce an AME(6,2).

We can then analyze the bipartitions of the 12-qubit state, either local or non-local. The resulting reduced density matrices to 6 qubits carry entropies that range from 4 to 6.

REED-SOLOMON CODES FOR EACH PLATONIC SOLID

Reed-Solomon codes offer the possibility of constructing fully AME states [30]. It is though clear that such codes do not make any use of the specific geometry of the dodecahedron. They just depend on the number of d -dimensional degrees of freedom placed on n sites. In particular, Reed-Solomon codes exist for states with $d = p$ a prime number, and $n = p + 1$. This fact combines smoothly with the 5 platonic solids, since in all cases, the

Tetrahedron	Faces = 4	AME(4,3)
Tetrahedron	Edges = 6	AME(6,5)
Tetrahedron	Vertices = 4	AME(4,3)
Exahedron	Faces = 6	AME(6,5)
Exahedron	Edges = 12	AME(12,11)
Exahedron	Vertices = 8	AME(8,7)
Octahedron	Faces = 8	AME(8,7)
Octahedron	Edges = 12	AME(12,11)
Octahedron	Vertices = 6	AME(6,5)
Dodecahedron	Faces = 12	AME(12,11)
Dodecahedron	Edges = 30	AME(30,29)
Dodecahedron	Vertices = 20	AME(20,19)
Icosahedron	Faces = 20	AME(20,19)
Icosahedron	Edges = 30	AME(30,29)
Icosahedron	Vertices = 12	AME(12,11)

TABLE III: All platonic solids carry a number of Faces, Edges and Vertices which are a prime number plus one. Thus, a Reed-Solomon code can be associated to each construction.

number of vertices, edges and faces are a prime number plus one.

Let us illustrate the example of AME(12,11), such that the minimal Hamming distance between any pair of elements in the set is $d_H = 7$. We first need to create the Reed-Solomon generating matrix, made with increasing powers of integers 1 to 10, all mod(11),

$$G = \begin{pmatrix} 1 & 1 & 1 & 1 & 1 & 1 & 1 & 1 & 1 & 1 & 0 \\ 0 & 1 & 2 & 3 & 4 & 5 & 6 & 7 & 8 & 9 & 10 & 0 \\ 0 & 1 & 4 & 9 & 5 & 3 & 3 & 5 & 9 & 4 & 1 & 0 \\ 0 & 1 & 8 & 5 & 9 & 4 & 7 & 2 & 6 & 3 & 10 & 0 \\ 0 & 1 & 5 & 4 & 3 & 9 & 9 & 3 & 4 & 5 & 1 & 0 \\ 0 & 1 & 10 & 1 & 1 & 1 & 10 & 10 & 10 & 1 & 10 & 1 \end{pmatrix}. \quad (18)$$

We then create all the elements of the superposition of AME(12,11) by taking each element of a basis x_i for 6 11-dits and compute $a_i = x_i \cdot G$. These numbers become the coefficients of the AME state,

$$|\text{AME}(12, 11)\rangle = \frac{1}{\sqrt{11^6}} \sum_{i=1, \dots, 11^6} |a_i\rangle. \quad (19)$$

The result is a state which is maximally entangled in all its partitions, and with a minimum Hamming distance 7 among each pair of superposed elements.

In general, the AME(n, p) with $n = p + 1$ is obtained following a similar procedure. The elements of the superposition are obtained as the images of all elements of $n/2$ bits. The minimal Hamming distance is then $\frac{n}{2} + 1$.

CONCLUSION

TN based on multipartite entangled ancillary states can be used to deploy entanglement on different topolo-

gies. We have here shown how these states define very highly entangled states for the case of using AME ancillary states on platonic solids. The quantum states constructed in this manner are locally fully entangled and achieved very large entanglement on arbitrary partitions.

It is a remarkable fact that all platonic solids have a number of faces, edges and vertices corresponding to a prime number plus one. It follows that they all accept AME related to Reed-Solomon error correcting codes as the ancillary building blocks of the TN structure.

Acknowledgements.

GS acknowledges support from the grants PGC2018-095862-B-C21, QUITEMAD+ S2013/ICE-2801, SEV-2016-0597 of the *Centro de Excelencia Severo Ochoa* Programme and the CSIC Research Platform on Quantum Technologies PTI-001.

-
- [1] F. Verstraete, J. I. Cirac, V. Murg, “Matrix Product States, Projected Entangled Pair States, and variational renormalization group methods for quantum spin systems”, *Adv. Phys.* **57**,143 (2008).
 - [2] R. Orús, “A practical introduction to tensor networks: Matrix product states and projected entangled pair states”, *Ann. Phys.* **349**, 117 (2014).
 - [3] G. Vitagliano, A. Riera, and J. I. Latorre, “Violation of area-law scaling for the entanglement entropy in spin 1/2 chains”, *New J. Phys.* **12**, 113049 (2010).
 - [4] G. Ramírez, J. Rodríguez-Laguna, G. Sierra, “Entanglement over the rainbow”, *J. Stat. Mech.* (2015) P06002.
 - [5] D. Alsina and J. I. Latorre, “Tensor networks for frustrated systems: emergence of order from simplex entanglement”, arXiv:1312.0952.
 - [6] A. García-Sáez and J. I. Latorre, “An exact tensor network for the 3SAT problem”, *Quant. Inf. and Comp.* **12**, 0283 (2012).
 - [7] W. Helwig, W. Cui, A. Riera, J. I. Latorre and H-K. Lo, “Absolute maximal entanglement and quantum secret sharing”, *Phys. Rev. A* **86**, 052335 (2012).
 - [8] W. Helwig and W. Cui, “Absolutely maximally entangled states: Existence and applications”, arXiv:quant-ph/1306.2536 (2013).
 - [9] D. Goyeneche and K. Życzkowski, “Genuinely multipartite entangled states and orthogonal arrays”, *Phys. Rev. A* **90**, 022316 (2014).
 - [10] D. Goyeneche, D. Alsina, J. I. Latorre, A. Riera, K. Życzkowski, “Absolutely Maximally Entangled states, combinatorial designs and multi-unitary matrices”, *Phys. Rev. A*, **92**, 032316 (2015).
 - [11] Z. Raissi, C. Gogolin, A. Riera, A. Acín, “Optimal quantum error correcting codes from absolutely maximally entangled states”, *J. Phys. A* **51**, 075301 (2018).
 - [12] A. J. Scott, “Multipartite entanglement, quantum-error-correcting codes, and entangling power of quantum evolutions”, *Phys. Rev. A* **69**, 052330 (2004).

- [13] F. Huber, O. Gühne, and J. Siewert, “Absolutely maximally entangled states of seven qubits do not exist”, *Phys. Rev. Lett.*, **118**, 502 (2017).
- [14] A. Bernal, “On the Existence of Absolutely Maximally Entangled States of Minimal Support”, *Quant. Phys. Lett.* **6**, 1, 2017.
- [15] A. Bernal, “On the Existence of Absolutely Maximally Entangled States of Minimal Support II”, arXiv:1807.00218 (2018).
- [16] F. Huber, C. Eltschka, J. Siewert, O. Gühne, “Bounds on absolutely maximally entangled states from shadow inequalities, and the quantum MacWilliams identity”, *J. Phys. A: Math. Theor.* **51**, 175301 (2018).
- [17] A. Cervera-Lierta, J. I. Latorre, D. Goyeneche, “Quantum circuits for maximally entangled states”, *Phys. Rev. A* **100**, 022342 (2019).
- [18] D. Alsina, M. Razavi, “Absolutely maximally entangled states, quantum maximum distance separable codes, and quantum repeaters”, *Phys. Rev. A* **103**, 022402 (2021).
- [19] J. I. Latorre and G. Sierra, “Holographic Codes”, arXiv:1502.06618 (2015).
- [20] F. Pastawski, B. Yoshida, D. Harlow and J. Preskill, “Holographic quantum error-correcting codes: Toy models for the bulk/boundary correspondence”, *JHEP* **06**, 149 (2015).
- [21] D. Harlow, “The Ryu-Takayanagi Formula from Quantum Error Correction”, arXiv:1607.03901, (2016).
- [22] P. Hayden, S. Nezami, X.-L. Qi, N. Thomas, M. Walter, Z. Yang, “Holographic duality from random tensor networks”, arXiv:1601.01694 (2016).
- [23] A. Jahn, J. Eisert, “Holographic tensor network models and quantum error correction: A topical review”, arXiv:2102.02619 (2021).
- [24] A. Tavakoli and N. Gisin, “The Platonic solids and fundamental tests of quantum mechanics”, *Quantum* **4**, 293 (2020).
- [25] A. Jadczyk, R. Oberg, “Quantum Jumps, EEQT and the Five Platonic Fractals”, arXiv:quant-ph/0204056 (2002).
- [26] T. Decker, D. Janzing, T. Beth, “Quantum circuits for single-qubit measurements corresponding to platonic solids”, *Int. J. Quan Inf.* **02**, 353 (2004).
- [27] P. Kolenderski, R. Demkowicz-Dobrzanski, “Optimal state for keeping reference frames aligned and the Platonic solids”, *Phys. Rev. A* **78**, 052333 (2008).
- [28] M. Burrello, H. Xu, G. Mussardo, X. Wan, “Quantum hashing with the icosahedral group”, *Phys. Rev. Lett.* **104**, 160502 (2010).
- [29] K. Bolonek-Lasoń, P. Kosiński, “Groups, Platonic solids and Bell inequalities”, arXiv:2009.04347.
- [30] I. S. Reed and G. Solomon, “Polynomial codes over certain finite fields”, *J. Soc. Indust. Appl. Math.* **8**, 300 (1960).